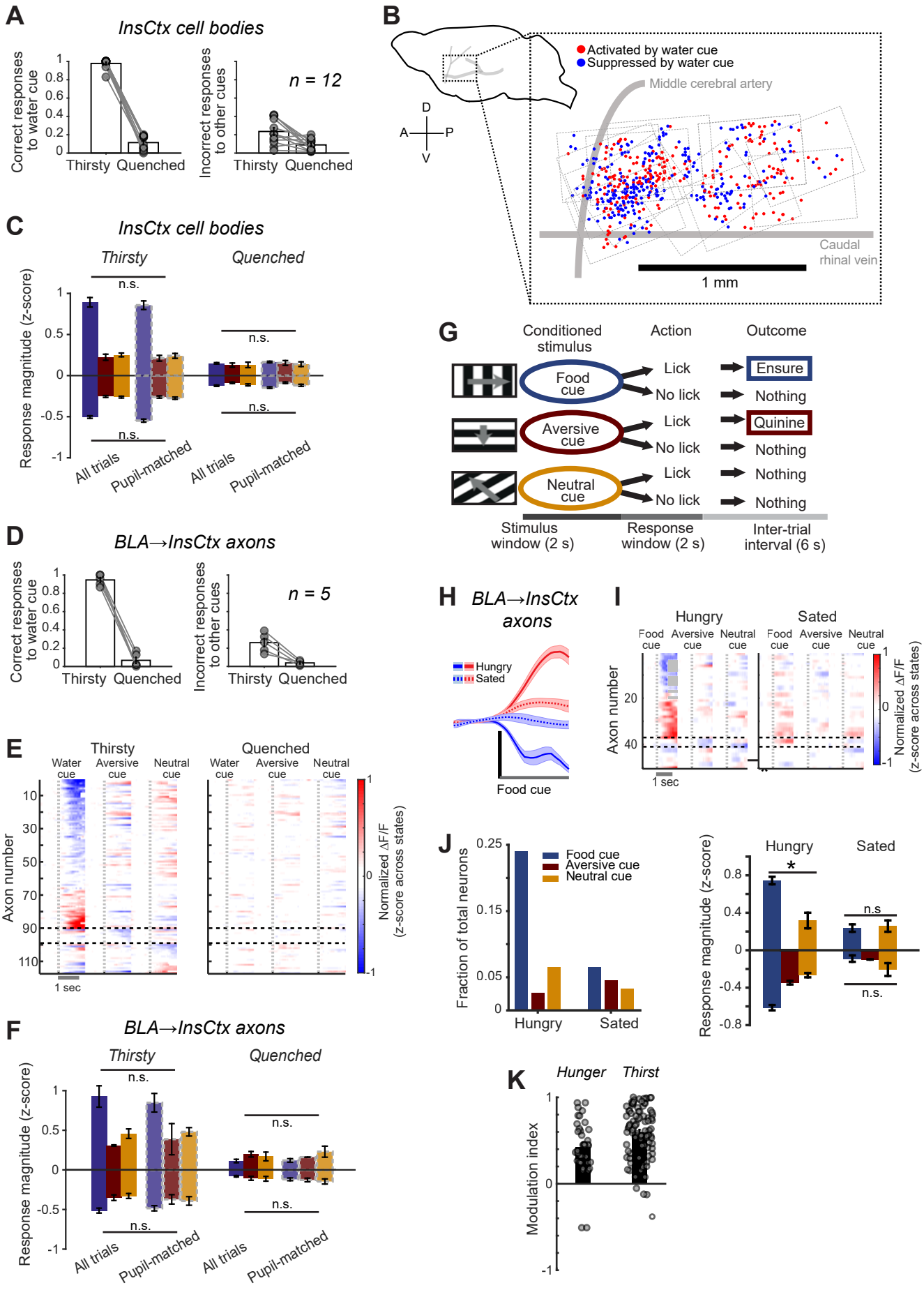
A
InsCtx cell bodies
Correct responses to water cue
Thirsty Quenched
Incorrect responses to other cues
n = 12
B
Activated by water cue
Suppressed by water cue
Middle cerebral artery
Caudal rhinal vein
1 mm
C
InsCtx cell bodies
Thirsty
Quenched
Response magnitude (z-score)
n.s.
All trials
Pupil-matched
G
Conditioned stimulus
Action
Outcome
Food cue
Aversive cue
Neutral cue
Lick
No lick
Ensure
Quinine
Nothing
Stimulus window (2 s)
Response window (2 s)
Inter-trial interval (6 s)
D
BLA→InsCtx axons
n = 5
H
BLA→InsCtx axons
Hungry
Sated
Food cue
I
Hungry
Sated
Axon number
Normalized ΔF/F (z-score across states)
1 sec
E
Thirsty
Quenched
Water cue
Aversive cue
Neutral cue
J
Fraction of total neurons
Food cue
Aversive cue
Neutral cue
Hungry
Sated
Response magnitude (z-score)
F
BLA→InsCtx axons
K
Hunger
Thirst
Modulation index

Supp. Fig. S1

Figure S1, Related to Figure 1: Behavior across Thirsty and Quenched States; Controls for Arousal across States; Additional BLA→InsCtx Axon Imaging Data

A. Summary of behavior across mice used for InsCtx cell body imaging. Correct responses for trials involving water cues contained at least one lick response in the 2-sec window following cue offset. Incorrect responses for trials involving other cues contained at least one lick response in the 2-sec window following cue offset.

B. *Left:* schematic side view of the mouse brain, highlighting the location of the caudal rhinal vein (CRV) and middle cerebral artery (MCA). *Right:* anatomical location of all imaged neurons (dots), relative to the CRV and MCA junction, showing no spatial bias of neurons activated (red) or suppressed (blue) by water cues. Dashed rectangles show the borders of each imaging field of view. A: anterior, P: posterior, D: dorsal, V: ventral.

C. Differential arousal levels do not explain differences in InsCtx neuronal responses across thirsty and quenched states. Comparison of InsCtx cue responses when matching pupil diameter (as a proxy for ongoing arousal levels) across states, or not matching. Matching pupil diameter in each state involved sub-selecting sets of trials with matching distributions of pre-cue pupil diameter. Note that there is no difference between cue response magnitudes estimated using all trials vs. pupil-matched trials. n.s.: not significant, $p>0.17$ for all cues and states (all trials vs. pupil-matched), Mann-Whitney test. *Activated neurons:* n = 144, 8, 13 neurons responsive to the water, aversive, and neutral cue, respectively. *Suppressed neurons:* n = 195, 73, 77 neurons responsive to the water, aversive, and neutral cue, respectively.

D. Summary of behavior across mice used for BLA→InsCtx axon imaging in water-restricted (thirsty) mice.

E. Heatmap of the average neuronal responses to the 3 visual cues during thirsty and quenched states for all cue-responsive axons. Vertical dashed lines: visual cue onset. Horizontal dashed lines: separation between sets of axons, grouped by the cue that evoked the strongest response.

F. Differential arousal levels do not explain differences in BLA→InsCtx axon responses across thirsty and quenched states. Comparison of cue responses when matching pupil diameter (as a proxy for ongoing arousal levels) across states, or not matching. Note that there is no difference between cue response magnitudes estimated using all trials vs. pupil-matched trials. n.s.: not significant, $p>0.33$ for all cues and states, Mann-Whitney test. *Activated:* n = 26, 2, 14 axons responsive to the water, aversive, and neutral cue, respectively. *Suppressed:* n = 66, 12, 13 axons responsive to the water, aversive, and neutral cue, respectively.

G. Schematic of the visual discrimination task for food-restricted (hungry) mice.

H. Average BLA→InsCtx axon population responses to the food cue during hungry (solid lines) and sated (dashed lines) states. Scale bar: 0.4 normalized $\Delta F/F$ (z-score across states). Values are mean±s.e.m; n=37 cue-responsive axons. Axons activated or suppressed by the food cue are red and blue, respectively.

I. Heatmap of the average neuronal responses to the 3 visual cues during hungry and sated states for all cue-responsive axons. Vertical dashed lines: visual cue onset. Horizontal dashed lines: separation between sets of axons, grouped by the cue that evoked the strongest response. Missing values (gray) are time-points with too few trials without licking to be used for averaging across trials (see Methods).

J. Quantitative analyses of cue-responsive axons across hunger and satiety. *Left:* fraction of all recorded axons (n=157 axons from 3 mice) responsive to each visual cue, revealing a bias to the food cue. *Right:* average response magnitude across hungry and sated states. Note that the response bias to the food cue is abolished following satiation. *$p=4.8\times10^{-5}$ (Hungry, suppressed), *$p=0.005$ (Hungry, activated), ns: not significant ($p>0.7$, Sated for both activated and suppressed), Kruskal-Wallis test. Pairwise comparisons between cues (Hungry, both excited and suppressed): $p\leq0.006$, Mann-Whitney test (axons responding to the food, aversive and neutral cues: suppressed: n= 19, 4 and 6, excited: n= 18, 0, and 4, respectively; from 3 mice).

K. Comparison of modulation index between hungry/sated and thirsty/quenched states in BLA→InsCtx axons. Note higher modulation index (mean ± s.e.m.) for thirsty/quenched vs. hungry/sated. *$p = 0.006$, Mann-Whitney test, n= 37 and 92 axons for hungry/sated and thirsty/quenched state, respectively.

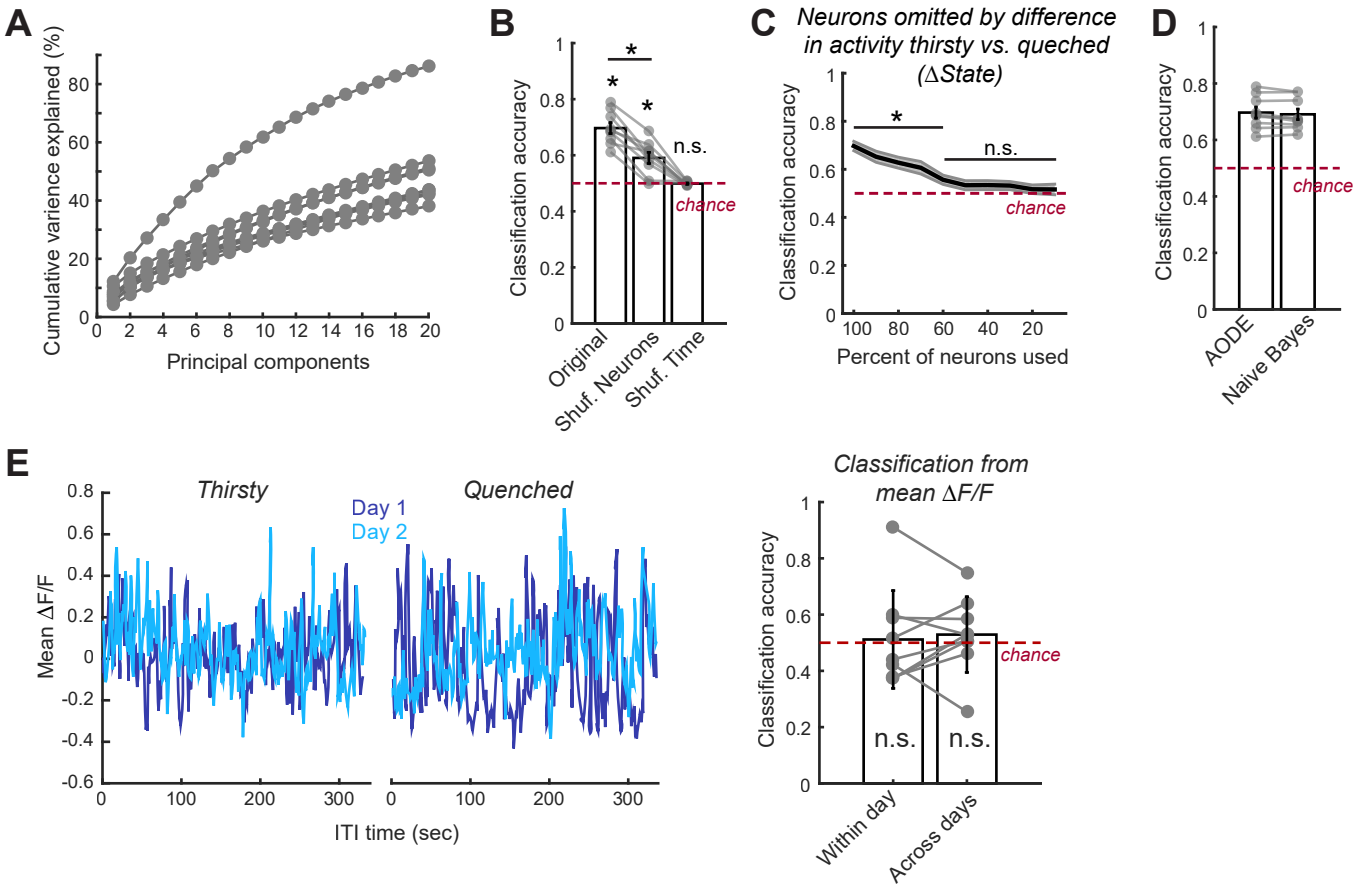

Figure S2, Related to Figure 2: Further Analyses of Ongoing Activity across Thirsty and Quenched States.

A. Cumulative variance explained by principal components for all 9 FOVs using principal component analysis.

B. Classification accuracy of thirsty vs. quenched states across days after shuffling neuron labels or shuffling in time by randomizing the order of population activity vectors at each time point. Note that classification remained significantly above chance after shuffling neurons, but not time. *p≤0.004, n.s.: not significant, p=0.58, t-test vs. chance, n=9 FOVs from 7 mice.

C. Classification accuracy after gradual omission of neurons, ordered by how informative each neuron was for classification, from most informative (left) to least informative (right). In other words, neurons were ordered by descending magnitudes of ΔState – the average normalized difference in ongoing activity between thirsty vs. quenched states. ΔState is proportional to a cell's classifier weight. *p<0.05, n.s.: not significant, t-test vs. chance with Holm-Bonferroni correction for multiple comparisons, n=9 FOVs from 7 mice.

D. Comparison between classification accuracy using an AODE classifier or a Naïve Bayes classifier. Note that the AODE classifier accounts for pairwise correlations in activity, while the Naïve Bayes classifier does not.

E. Mean ongoing activity is not sufficient to classify thirsty vs. quenched states. *Left:* example mean activity across all neurons from one mouse, thirsty vs. quenched, across two consecutive days. *Right:* classification accuracy within-day and across-days when using mean activity averaged across all neurons per FOV. n.s.: not significant, p≥0.54, t-test vs. chance, n=9 FOVs from 7 mice.

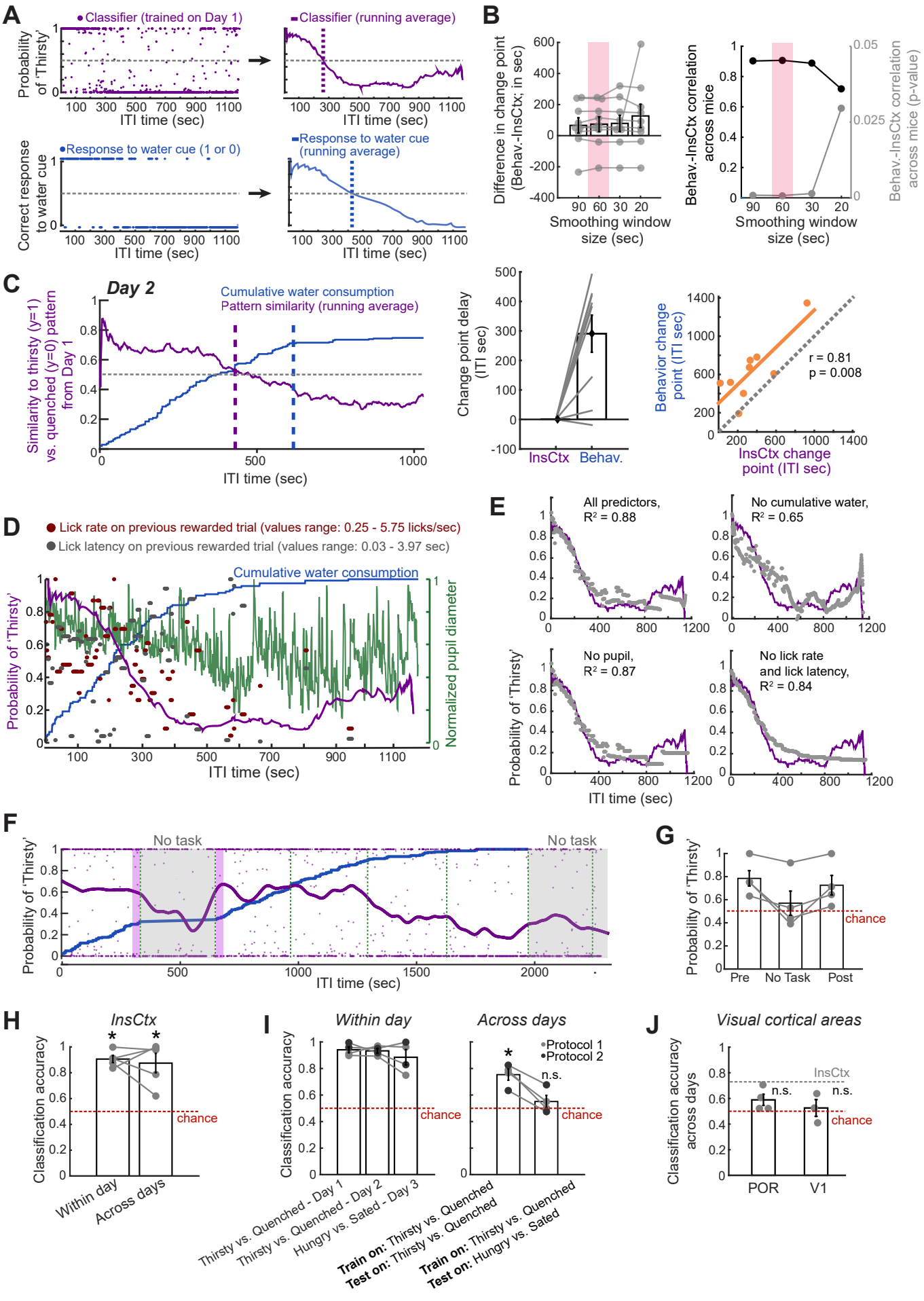
A
Classifier (trained on Day 1)
Classifier (running average)
Probability of 'Thirsty'
ITI time (sec)
Response to water cue (1 or 0)
Response to water cue (running average)
Correct response to water cue
B
Difference in change point (Behav.-InsCtx; in sec)
Smoothing window size (sec)
Behav.-InsCtx correlation across mice
Behav.-InsCtx correlation across mice (p-value)
C
Day 2
Cumulative water consumption
Pattern similarity (running average)
Similarity to thirsty (y=1) vs. quenched (y=0) pattern from Day 1
Change point delay (ITI sec)
InsCtx
Behav.
Behavior change point (ITI sec)
InsCtx change point (ITI sec)
r = 0.81
p = 0.008
D
Lick rate on previous rewarded trial (values range: 0.25 - 5.75 licks/sec)
Lick latency on previous rewarded trial (values range: 0.03 - 3.97 sec)
Cumulative water consumption
Probability of 'Thirsty'
Normalized pupil diameter
E
All predictors, R² = 0.88
No cumulative water, R² = 0.65
No pupil, R² = 0.87
No lick rate and lick latency, R² = 0.84
F
No task
No task
G
chance
Pre
No Task
Post
H
InsCtx
Classification accuracy
chance
Within day
Across days
I
Within day
Across days
Protocol 1
Protocol 2
n.s.
Thirsty vs. Quenched - Day 1
Thirsty vs. Quenched - Day 2
Hungry vs. Sated - Day 3
Train on: Thirsty vs. Quenched
Test on: Thirsty vs. Quenched
Train on: Thirsty vs. Quenched
Test on: Hungry vs. Sated
J
Visual cortical areas
Classification accuracy across days
InsCtx
n.s.
chance
POR
V1

Supp. Fig. S3

Figure S3, Related to Figure 3: Further Analyses Demonstrating that InsCtx Ongoing Activity Reflects Physiological State.

A. Method used for identifying a transition from a thirsty to a quenched state for the classifier (*top*) and for task engagement (*bottom*), following smoothing with a 60-sec running average. Note that the estimated time of state transition (change point) to a quenched state (top) and to a behaviorally disengaged state (bottom) was defined as the time when the smoothed time course dropped below a probability of 0.5 (horizontal dashed gray lines). Same data as in **Figure 3A**. See Methods for details. ITI time: time within the timeseries of concatenated time series for all selected ITIs.

B. Analyses using different sizes of the smoothing window yielded similar results. *Left:* difference in change point between behavioral engagement (bottom plots in **A**) and InsCtx activity-based classifier (top plots in **A**). Gray dots: individual mice. *Right:* R-values and p-values for the correlation between classifier change point and behavioral change point. Pink shaded area indicates the window size used for analyses in Figure 3.

C. Assessment of the relationship between InsCtx ongoing activity and task engagement using an alternative approach based on pattern similarity, rather than classification. *Left:* example pattern similarity of Day 2 ongoing activity during an entire recording session to Day 1 Thirsty vs. Quenched ongoing activity. Note that ongoing activity becomes more similar to a quenched state long before changes in behavior. *Middle:* difference between pattern similarity-predicted and actual change points from Thirsty to Quenched (i.e., between dashed purple and blue lines in the left panel) for all experiments. *Right:* correlation between the two change points across all experiments. Note qualitative similarity between these results and the ones in **Figure 3**.

D-E. Example of predicting InsCtx ongoing activity (as captured by classifier dynamics) from (1) amount of water consumed, (2) pupil diameter, (3) lick response latency on the most recent rewarded trial, and (4) lick rate on the most recent rewarded trial (same example in **Figure 3D**).

D. Example of parameters used for predicting InsCtx ongoing activity (as captured by classifier dynamics). Same example shown in **Figure 3**.

E. Prediction of InsCtx ongoing activity dynamics using all predictors or using subsets of predictors. Same example as in **Figure 3**. Note that omitting cumulative water rewards causes the largest decrease in variance explained by the model fit (i.e., R^2). Purple lines: real ongoing activity dynamics (classifier probabilities). Gray dots: predicted ongoing activity dynamics.

F-G. InsCtx ongoing activity does not reflect time elapsed.

F. Example data from a mouse imaged during 10-minute periods of disengagement between task epochs (periods in which water was not available and no cues were presented, highlighted in gray), thereby decoupling time elapsed during the session from amount of water consumed. Shaded purple areas: times before (pre) and after (post) no-task periods, used for analysis in **G** (20 sec of 'ITI time' using concatenation of selected ITIs, corresponding to ~2 min of 'real time').

G. Comparison of classification accuracy during the no-task periods and in the 20 seconds of ITI time before (pre) and after (post) no-task periods. Note that upon re-engagement in the behavioral task, classification returned to previous levels.

H. Classification accuracy of hungry vs. sated states from InsCtx ongoing activity. *p≤0.007, t-test vs. chance, n=5 mice.

I. Specificity of InsCtx ongoing activity pattern reflecting either thirsty or hungry states. We used two different 3-day protocols that yielded similar results (see Methods). In both protocols, Days 1-2 involved thirsty and quenched states (and a cue predicting water delivery), while Day 3 involved hungry and sated states (and a cue predicting liquid food delivery). *Left*: classification accuracy was high for within-day classification on all 3 days. *p≤0.007, t-test, n=4 mice. *Right:* across-day classification when training the classifier on thirsty/quenched states from Day 2 and then testing it on thirsty/quenched data from Day 1 (left bar) or hungry/sated data from Day 3 (right bar). Note that, despite equal times between training data (Day 2) and testing data (Days 1 or 3), classification accuracy was above chance only when training *and* testing the classifier on thirsty/quenched activity, suggesting that InsCtx ongoing activity is distinct for different deficiency states. *p=0.009, n.s.: not significant, p=0.34, t-test vs. chance, n=4 mice. Note that we were equally successful, in other experiments, in training a classifier on hungry/sated states and testing on hungry/sated data from a subsequent session (see **H**). Thus, this finding is not due to a general inability to use a classifier to classify hungry states across days.

J. Hungry vs. sated states cannot be classified from ongoing activity in two other cortical areas, primary visual cortex (V1) and postrhinal visual association cortex (POR). n.s.: not significant, p≥0.13, t-test vs. chance, n=4 mice for POR (49±7 neurons per mouse) n=3 mice for V1 (38±21 neurons per mouse), respectively. Because the number of neurons per mouse is lower than InsCtx populations, we randomly sub-selected a similar number of InsCtx neurons for comparison of across-day classification (dashed horizontal line).

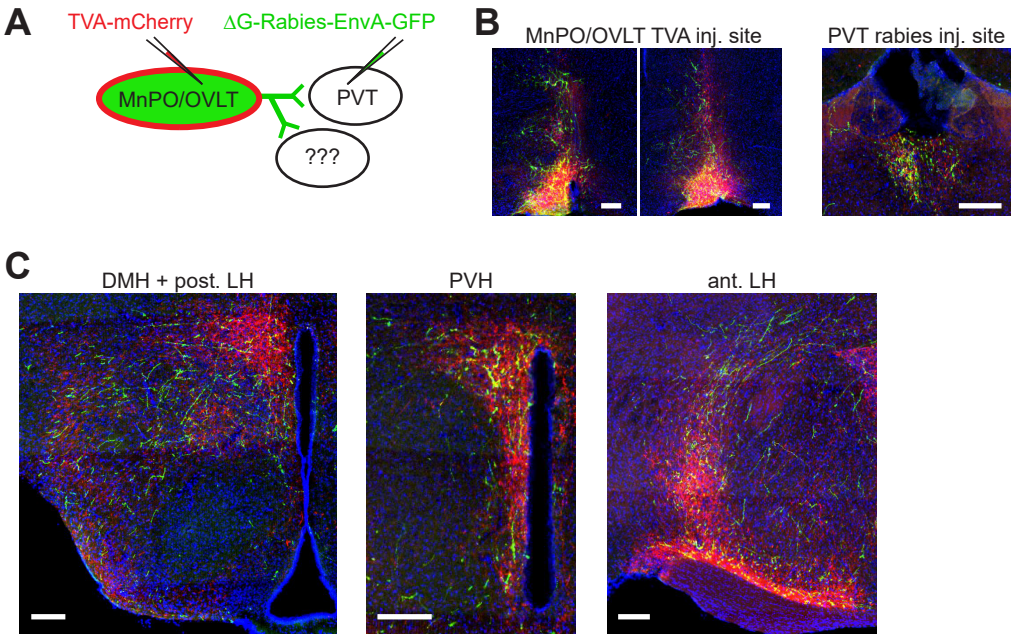

<u>Figure S4, Related to Figure 4</u>: MnPO^{GLUT}→PVT collateral mapping

A. Rabies-based axon collateral mapping approach for MnPO^{GLUT}→PVT.

B. *Left*: image of the TVA-mCherry injection site in MnPO/OVLT, containing neurons labeled with TVA-mCherry (red) and rabies (green). *Right*: image of the rabies injection site in the PVT (infecting MnPO^{GLUT}→PVT axons). Scale bars: 200 μm.

C. Labeled axons were found in anterior and posterior lateral hypothalamus (LH), in dorsomedial hypothalamus (DMH), and in paraventricular hypothalamus (PVH). Scale bars: 200 μm.

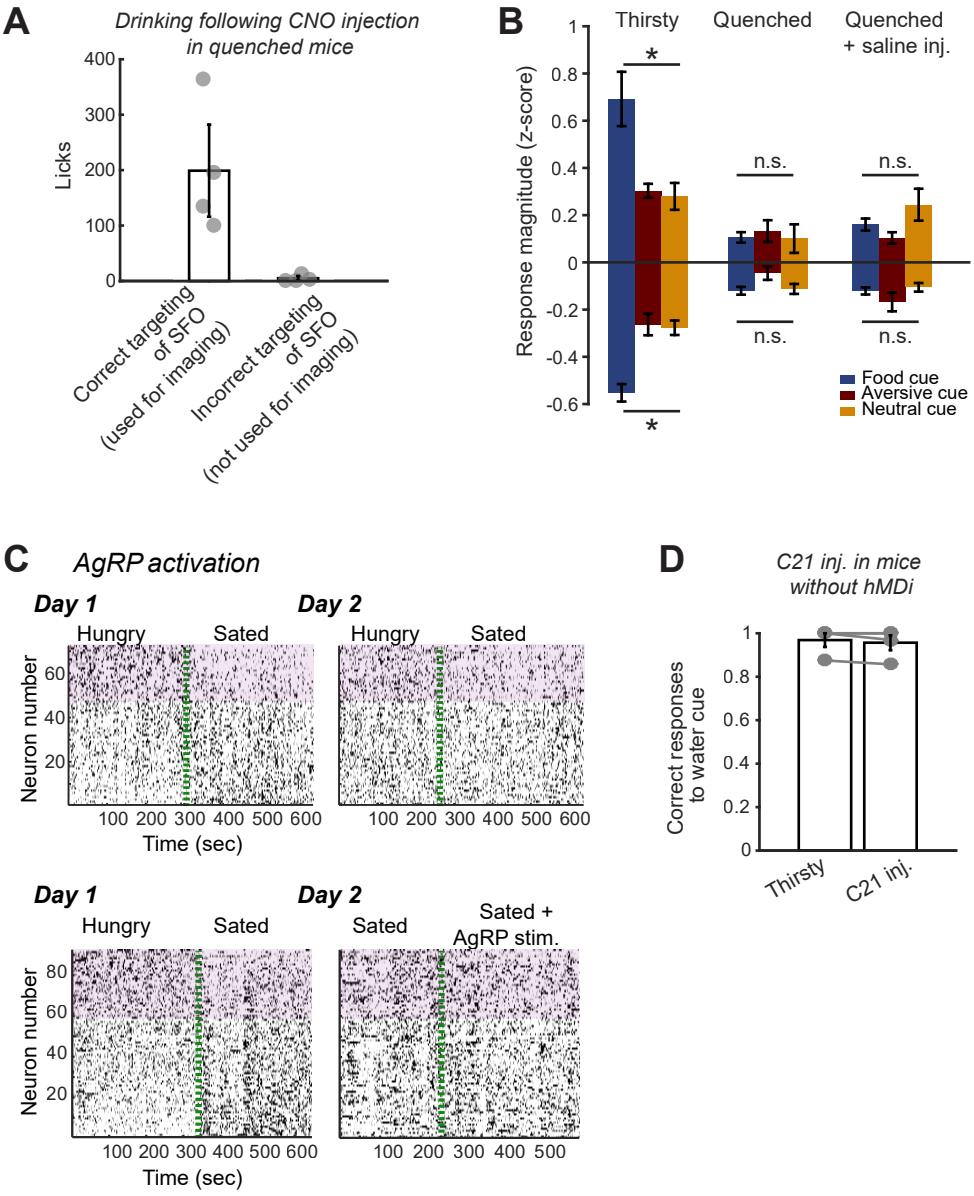

<u>Figure S5, Related to Figures 5 and 6</u>: Control Experiments for SFO^{GLUT} Activation and MnPO^{GLUT} Inhibition; Ongoing activity with AgRP activation

A. CNO injections in the absence of hM3Dq do not induce drinking. Comparison of drinking in mice with hM3Dq expression in SFO^{GLUT} neurons (n = 4 mice), and mice without hM3Dq expression (n = 5 mice). CNO injection induced drinking only in mice with hM3Dq expression in SFO^{GLUT} neurons.

B. Intraperitoneal saline injections do not mimic thirst in InsCtx. Average response magnitude of InsCtx neurons across Thirsty, Quenched, and Quenched + saline injections (n=98 neurons from 3 mice,). *p<0.03 (Thirsty, differences between cue responses, activated and suppressed), n.s.: not significant (p≥0.6, Quenched, Quenched+saline inj., differences between cue response), Kruskal-Wallis test.

C. Ongoing activity across 'Hungry', 'Sated', and 'Sated + AgRP activation' states. *Top:* example ongoing activity during hunger and satiety across two consecutive days. *Bottom:* example ongoing activity during hungry and sated states on Day 1, and then during satiety and AgRP activation on the following day. Note that hungry/sated runs were concatenated, and in practice are separated by a ~1 hr satiation protocol.

D. C21 injections do not affect performance in the visual discrimination task. Comparison of correct behavioral responses to water cues in mice without hM4Di expression across saline and C21 injections: p=0.21 (paired t-test), n = 4 mice.

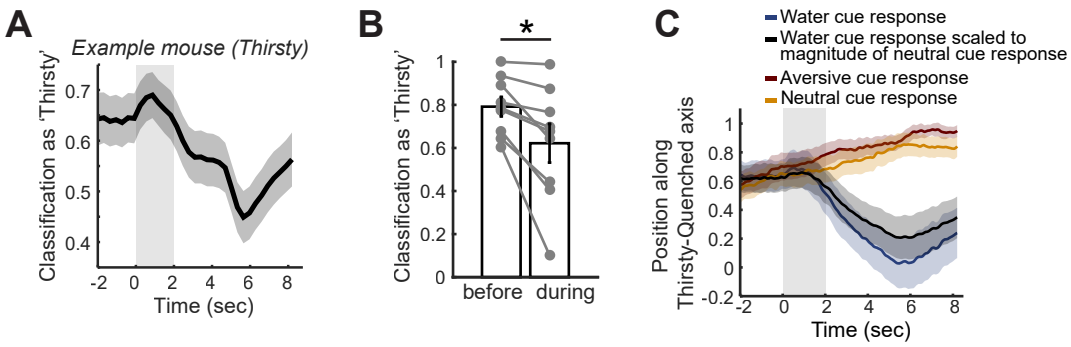

<u>Figure S6, Related to Figure 7</u>: Further Analyses Demonstrating that InsCtx Responses to Cues and Consumption Resemble a Future Satiety State

A. Example mean classification probability of population activity as thirsty vs. quenched (classifier trained on thirsty vs. quenched epochs of ongoing activity), both during presentation of a water cue and subsequent water consumption. Mean±s.e.m. of 45 cue presentations. Gray shaded area: cue period. Note that activity levels were not normalized to the pre-cue period prior to classification.

B. Comparison of classification of InsCtx activity patterns before vs. after water cue onset as in the example in **C**, but for all datasets (classifier trained on thirsty vs. quenched epochs of ongoing activity). *p=0.003, paired t-test (n=9 datasets from 7 mice).

C. As illustrated in the schematic in **Figure 7A**, we projected the time-varying peri-cue patterns (in N-dimensional space, where N is the number of simultaneously recorded InsCtx neurons, illustrated here in 3 dimensions) along the axis (gray line in **Figure 7A**) that connects ongoing activity patterns in the thirsty state (blue cloud in **Figure 7A**, with patterns corresponding to values near 1) to those in the quenched state (yellow cloud in **Figure 7A**, with patterns corresponding to values near 0). This yielded a scalar value of 'position along the Thirsty-Quenched axis', reflecting relative similarity of a pattern to the Thirsty vs. Quenched states. Patterns beyond this quenched state along the same axis correspond to a negative value, possibly reflecting actual or predicted overconsumption.

This is the same plot as in **Figure 7D**, but including a version (black line) of the water cue response pattern along the thirsty vs. quenched axis after scaling the magnitude of the population responses to the substantially weaker magnitude responses to the neutral cue. This controls for non-specific changes that might simply be due to larger (and thus potentially higher signal-to-noise) population responses regardless of pattern. This analysis suggests that, in the thirsty state, water cues and associated consumption (but not other types of cues) evoke a shift of population activity towards a quenched state, and that this shift is due to the specific water cue-evoked pattern of activity and not due to the larger magnitude of responses to water cues vs. other cues.